CI&CEQ
Chemical Industry & Chemical Engineering Quarterly

Available on line at
Association of the Chemical Engineers of Serbia *AChE*
www.ache.org.rs/CICEQ

Chem. Ind. Chem. Eng. Q. 24 (4) 345–356 (2018) CI&CEQ

HONDA WU

Department of Fashion styling and Design, Chungyu University of Film and Arts, Keelung, Taiwan, R.O.C.

SCIENTIFIC PAPER

UDC 66.081.3:546.264-31

PARTICULATE AND MEMBRANE MOLECULAR SIEVES PREPARED TO ADSORB CARBON DIOXIDE IN PACKED AND STAGGERED ADSORBER

Article Highlights

- Carbon dioxide was removed by the staggered adsorption system successful
- The adsorption capacity can be quickly obtained from microbalance adsorption system
- The configuration of molecular sieve was affected by the rate of hydrolysis
- The staggered system with coating molecular sieve is worthy to be developed
- Adsorption of carbon dioxide by molecular sieve is better than methane

Abstract

A fixed-bed adsorption system was used to remove carbon dioxide in this study. Adsorption isotherms were obtained from a microbalance system and the characteristics of a molecular sieve affected by preparing variables were analyzed. The adsorbents, including a particulate molecular sieve and a molecular sieve membrane, were used to adsorb carbon dioxide in the fixed-bed adsorption system. Since the surface properties of the molecular sieve were affected by the preparation variables, particulate and membrane molecular sieves were synthesized to examine the effects of preparation variables on the adsorption of carbon dioxide. The experimental results showed that the pore size of the molecular sieve has increased with the chain length of quaternary ammonium salts and higher hydrothermal temperature. Adsorption isotherms for carbon dioxide adsorbed by particulate molecular sieve and molecular sieve membrane were favourable. In addition, the breakthrough curve for the lower inlet gas flow rate was closer to that of the particulate molecular sieve under the same amount of outlet fresh air. The results demonstrated that the adsorption system for the staggered alumina carriers coated with molecular sieve membranes is worthy of development.

Keywords: adsorption, carbon dioxide, microbalance, molecular sieve, regeneration.

Thermal power plants are among the largest sources of carbon dioxide emissions. During the combustion of fuels such as petroleum, natural gas, and coal, carbon combines with oxygen to form carbon dioxide. According to the International Energy Agency (IEA) [1], global CO_2 emissions in 2014 were 32.4 Gt CO_2, and the average annual growth rate in emissions since 2000 was 2.4%. Emissions of CO_2 in Annex I countries decreased by 1.8% due to modest declines in emissions from coal (-3.2%) and natural gas (-2.6%); however, those in non-Annex I countries increased by 2.5%. Global CO_2 emissions increased by 0.3 Gt CO_2 in 2014, and the increase in the emissions of non-Annex I countries was 66%, primarily from coal emissions. Since the growing energy demands of those developing countries are mostly met with coal, CO_2 emissions from the combustion of coal increased by 95% to 24.5 Gt CO_2 in 2014. Emissions of CO_2 from fossil fuel in 2014 were 34% from oil, 46% from coal, and 19% from gas. The current stra-

Correspondence: Department of Fashion styling and Design, Chungyu University of Film and Arts, No. 40, Yi-7th Rd., Keelung, Taiwan 20103, R.O.C.
E-mail: hungta.wu@msa.hinet.net
Paper received: 21 August, 2017
Paper revised: 3 March, 2018
Paper accepted: 27 March, 2018

https://doi.org/10.2298/CICEQ170821007W

tegy for reducing carbon dioxide emissions is to improve energy efficiency and to increase the use of renewable energy.

Previous studies have reported that the carbon dioxide adsorption performance of the molecular sieve is good [2-6]. The properties of a molecular sieve can be affected by the preparation conditions, modification of additives, pH-adjusting, and the substrate type or chemical treatment of the substrate. Therefore, the performance for adsorption of carbon dioxide can also be affected by them. For example, Wang *et al.* [3] fabricated molecular sieve membranes of different thickness and density by controlling the carbonization temperature. They found that the diffusion coefficient of CO_2 in these molecular sieve membranes had a functional dependence on the degree of carbonization. Ahmad *et al.* [7] varied the pyrolysis temperature, and their experiment in gas permeation found the highest CO_2 permeance in the sample prepared at 700 °C. Liao *et al.* [8] prepared carbon molecular sieve membranes (CMSMs) by carbonizing Kapton in a three-zone horizontal furnace. The preparation variables included pyrolysis temperature, heating rate, and holding time. Their experimental results demonstrated that the asymmetric microstructure of CMSMs decreases gas permeability and increases selectivity with a longer holding time. The properties of the molecular sieve can be modified by additives, as done in the preparation of PEI(polyethylenimine)-modified MCM-41 by Xu *et al.* [6] They found that the structure of the MEM-41 was preserved and the PEI was uniformly dispersed into the channels of the molecular sieve. Their results showed that the carbon dioxide adsorption capacity of PEI-modified MCM-41 was much greater than those of MCM--41 and pure PEI. In order to enhance the removal of methyl tert-butyl ether (MTBE) from aqueous solutions, Ghadiri *et al.* [9] added zeolitic-rich tuff to solutions containing hexadecyl trimethyl ammonium chloride and cetylpyridinium bromide. They found that the Langmuir isotherm was more suitable for fitting adsorption of MTBE by the modified zeolite and the removal efficiency was improved. The method of pH-adjusting was used by Shah *et al.* [10] to synthesize Copper-containing SBA-16 type molecular sieve. They found that pH 5 was the most suitable pH value to apply for adsorption desulfurization of dibenzothiophene (DBT). For treatment of substrate, Chau *et al.* [11] used acid treatment, deposition of metals and metal oxides, and adsorption of surfactant molecules to modify the property of the support surface. They demonstrated that iron(III) oxide promoted nucleation and the functional groups, -OH and -COOH, provided suitable nucleation sites for the zeolite. They also found that the adhesion of the zeolite membrane can be improved by surface micro-roughness, which can be controlled by acid treatment. Due to the high autogenous pressure associated with hydrothermal procedures, Li *et al.* [12] prepared aluminophosphate molecular sieve membranes on a porous substrate by ionothermal method, varying substrate type and solution composition.

Applications of molecular sieve membranes include carbon dioxide removal, separation of isomers, pervaporation, and reaction processes. Namba [13] prepared molecular sieve membranes to separate carbon dioxide in air and found that the separation performances of molecular sieve membranes and organic membranes were similar; however, the permeation rates of the synthetic membranes were 5 to 8.5 times that of the organic membrane. For isomers, separation of n-butane and iso-butane, *n*-hexane and iso-hexane, and *n*-octane and iso-octane have been the main focus. For example, a separation factor of 40 was obtained by Funke *et al.* [14] using Silicate-1 membrane to divide *n*-octane from iso-octane. A separation factor greater than 31 was obtained by Jia *et al.* [15] and Kapteijin *et al.* [16] using ZSM-5 and Silicate-1 membranes respectively to divide n-butane from iso-butane at a temperature of 185 °C. In addition to being used for separating alkanes, Silicate-1 membrane was also used by Kapteijin *et al.* [16] to examine its separation performance for aromatics. A zeolite membrane, ZSM-5/α-Al_2O_3, was synthesized by Ma and Xiang [17] to examine separation phenomena in the paraxylene/triisopropylbenzene mixed solution. For the pervaporation of liquid, a nano NaA zeolite membrane synthesized from kaolin was investigated by Kazemimoghadam [18]. From pervaporation of water-ethanol mixtures, the NaA zeolite membrane presented the higher water selectivity in the water-ethanol mixtures. In addition, zeolite-incorporated multilayer poly(vinyl alcohol) membranes were used by Huang *et al.* [19] to examine the pervaporation process for alcohol aqueous solution. For reaction processes, the dehydrogenation of alkane has been a focus. A ZSM-5 zeolite membrane was used by Zygmunt *et al.* [20] to examine the dehydrogenation of butane. In addition, a microporous silicalite zeolite membrane was used by Uzio *et al.* [21] to examine the dehydrogenation of iso-butane.

In addition to being resistant to high temperature, chemical attack, and biological corrosion, and having high mechanical strength and great flux, the molecular sieve also features surface properties that can be changed easily by altering the preparation

variables. For example, the silicon and aluminum atoms in the molecular sieve can be replaced with other atoms, and the ratio of silicon to metal can also be changed to control the surface properties. As mentioned above, the molecular sieve was used as adsorbent to capture carbon dioxide in this study. On the basis of the surface properties dependent on the preparation variables and the greater pressure drop resulted from filling with particulate adsorbent, the purpose of this study was to synthesize a molecular sieve to examine the effects of preparation variables on the surface characteristics of the molecular sieve, to set fixed-bed adsorbers packed with molecular sieve particulate and with the staggered molecular sieve membrane, and to test the performance of carbon dioxide adsorbed by them. Therefore, the surface characteristics of the molecular sieve particulate and membrane were checked and adjusted by variables such as the quaternary ammonium salts with different carbon-chain length, hydrothermal temperature, and addition of ethanol to find the molecular sieve suitable for adsorption of carbon dioxide.

EXPERIMENTAL

Preparation of molecular sieve particles and membranes

To discuss the effect of carbon-chain length on the synthesized molecular sieve, sodium silicate was used as a precursor and the quaternary ammonium salts with different carbon-chain length were used as a surfactant to prepare the molecular sieve. The quaternary ammonium salts used in this study included *n*-hexyltrimethylammonium bromide (C-6), *n*--octyltrimethylammonium bromide (C-8), tetradecyltrimethylammonium bromide (C-14) and octadecyl trimethyl ammonium bromide (C-16). In order to discuss the effect of hydrothermal temperature on the properties of molecular sieve, the hydrothermal temperatures were varied in this study. Therefore, 4.95 g quaternary ammonium salts were dissolved into 25.7 g deionized water at 45, 70 and 100 °C, respectively. Similarly, 9.2 g sodium silicate solution (35%) was dissolved into 9.2 g deionized water at 45, 70 and 100 °C to form sodium silicate aqueous solution. The quaternary ammonium salts aqueous solution were dropped slowly into the sodium silicate aqueous solution by a dropper, and the mixed solution was stirred for 25 min. Then 1 mol/L sulfuric acid was added slowly until the pH value reached 10. The polymer solution was sealed and stirred for 12 h at 45, 70 and 100 °C, respectively. After stirring, the polymer solution was heated in a water bath for 24 h at temperatures from 90 to 100 °C, and then the flocculated polymer solution was filtrated. The wet polymer filtrate was dried in an oven at 100 °C for 24 h. Finally, the polymer was placed into a furnace and heated at 500 °C for 2 h to obtain the particulate molecular sieve.

Previous studies have reported that adding ethanol shortens the spiral intercept of the spherical molecular sieve particles [22-24]. Generally speaking, the representation for the maximum surface tension is a circle, and the change in shape could be attributed to the decrease in surface tension. Since the addition of ethanol decreases the surface tension of the polymer solution, the molecular sieve particles become short and cylindrical in shape. Furthermore, the surface tension is the result of self-cohesion, and the lower self-cohesion should be advantageous to the process of membrane forming. Therefore, 0.6 g of ethanol was added to the surfactant aqueous solution to modify the properties of the molecular sieve membrane. Hydrothermal synthesis was used to prepare the molecular sieve membrane in this study. The precursor was the same as that for the particulate molecular sieve, and 0.6 g of ethanol was added to the quaternary ammonium salts aqueous solution. Alumina was used as the carrier, and the size of the carrier was 8 mm×8 mm×1 mm. The alumina carrier was placed inside the hydrothermal synthesis reactor, as shown in Figure 1. The polymer solution was heated to 45, 70 or 100 °C and then injected into the reactor until the carrier was submerged completely. To promote homogeneous growth of the molecular sieve membrane on the carrier, a hydrothermal synthesis reactor with rotating blades was set in the system. The whole hydrothermal synthesis system was placed inside the oven, and the temperature was controlled at 45, 70 or 100 °C for 2 h. The seed thus formed on

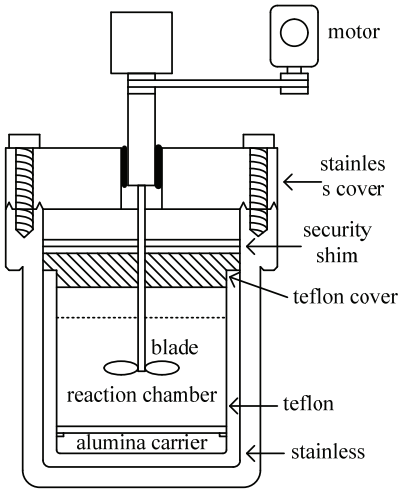

Figure 1. Hydrothermal reactor for this study.

the carriers due to the state of supersaturation. After the membrane was fabricated completely, the carriers coated with the molecular sieve membrane were rinsed with deionized water. Finally, they were dried at 120 °C for 2 h.

Adsorption test in microbalance and fixed-bed adsorption systems

The amount of carbon dioxide adsorbed by the molecular sieve was determined in two ways. One was in terms of adsorption capacity, measured by the microbalance adsorption system [25]. The advantage of using this system to obtain the adsorption capacity is the small amount of adsorbent needed. Unlike a traditional adsorption system, it does not require much time to conduct an adsorption test. In order to quickly determine the adsorption capacity with the microbalance adsorption system, the system was initially evacuated. The carbon dioxide pressure was controlled in the range from 0 to 1 MPa, and the temperature was maintained at room temperature (23–27 °C). When the weight reading on the microbalance stopped changing, the equilibrium state was reached and the reading was recorded to calculate the adsorption capacity. The adsorption amounts in Tables 1 and 2 were obtained from the adsorption test by the microbalance adsorption system.

The advantage of the microbalance adsorption system is that it saves time and energy as compared with the traditional fixed-bed adsorption tower. However, the breakthrough curve is not easy to accurately obtain from the microbalance adsorption system. In order to obtain breakthrough curves for carbon dioxide adsorbed by the synthesized molecular sieve, the fixed-bed adsorption system packed with the particulate molecular sieve was used to adsorb carbon dioxide in this study. Since the larger pressure drop would result in the fixed-bed adsorption system being packed with particulate particles, the alumina carriers coated with molecular sieve membranes were stag-

Table 1. Surface properties and adsorption data for molecular sieve membrane; data in parentheses mean without addition of ethanol

Sample	Hydrothermal temperature, °C	Surface area cm^2/g	Mesopore volume cm^3/g	Micropore volume cm^3/g	Pore size nm	Adsorption amount, CO_2 mg/g
C-6	45	1040 (996)	0.019 (0.018)	0.624 (0.533)	0.65 (0.75)	386 (345)
C-8	45	1022 (974)	0.024 (0.023)	0.604 (0.512)	0.95 (1.06)	377 (336)
C-14	45	870 (853)	0.582 (0.578)	0.032 (0.029)	2.75 (2.80)	297 (283)
C-16	45	851 (835)	0.566 (0.560)	0.026 (0.023)	3.02 (3.08)	281 (269)
C-6	70	1002 (953)	0.022 (0.021)	0.594 (0.502)	0.93 (1.04)	377 (333)
C-8	70	988 (940)	0.026 (0.025)	0.571 (0.480)	1.23 (1.33)	366 (323)
C-14	70	845 (829)	0.551 (0.545)	0.026 (0.023)	3.30 (3.35)	280 (267)
C-16	70	829 (812)	0.534 (0.527)	0.021 (0.019)	3.65 (3.71)	266 (252)
C-6	100	962 (916)	0.024 (0.023)	0.566 (0.471)	1.22 (1.33)	364 (321)
C-8	100	945 (898)	0.030 (0.028)	0.533 (0.439)	1.51 (1.63)	353 (308)
C-14	100	820 (803)	0.508 (0.501)	0.021 (0.018)	4.10 (4.16)	273 (259)
C-16	100	803 (788)	0.490 (0.480)	0.017 (0.015)	4.48 (4.54)	259 (246)

Table 2. Surface properties and adsorption data for particulate molecular sieve; data in parentheses mean without addition of ethanol

Sample	Hydrothermal temperature, °C	Surface area cm^2/g	Mesopore volume cm^3/g	Micropore volume cm^3/g	Pore size nm	Adsorption amount, CO_2 mg/g
C-6	45	1025 (978)	0.014 (0.013)	0.595 (0.503)	0.73 (0.81)	371 (329)
C-8	45	1008 (963)	0.020 (0.019)	0.573 (0.482)	1.02 (1.12)	363 (321)
C-14	45	858 (840)	0.570 (0.567)	0.026 (0.023)	2.81 (2.86)	285 (271)
C-16	45	840 (823)	0.553 (0.549)	0.021 (0.019)	3.10 (3.14)	269 (256)
C-6	70	989 (945)	0.018 (0.017)	0.565 (0.471)	1.02 (1.11)	360 (317)
C-8	70	975 (929)	0.021 (0.020)	0.540 (0.452)	1.30 (1.41)	351 (308)
C-14	70	830 (813)	0.538 (0.532)	0.021 (0.018)	3.41 (3.45)	268 (254)
C-16	70	812 (796)	0.519 (0.513)	0.016 (0.014)	3.75 (3.80)	255 (240)
C-6	100	948 (901)	0.020 (0.019)	0.535 (0.449)	1.31 (1.43)	348 (303)
C-8	100	930 (879)	0.025 (0.023)	0.505 (0.412)	1.60 (1.73)	338 (293)
C-14	100	804 (789)	0.492 (0.485)	0.017 (0.015)	4.21 (4.26)	257 (242)
C-16	100	787 (761)	0.473 (0.466)	0.012 (0.010)	4.60 (4.66)	243 (229)

gered in the adsorption system to adsorb carbon dioxide, as shown in Figure 2. The dimension of the adsorption tower was 10.3×10.3×100 mm^3, and 30 g of molecular sieve were used in the adsorption tower. According to the Material Safety Data Sheet, the permissible exposure limit 8-h time weighted average for carbon dioxide was 5000 ppm, the inlet concentration of carbon dioxide flowing into the fixed-bed adsorption system was controlled at 5000 ppm; that is, the mole ratio of air to carbon dioxide was 1:0.00278. The total volume flow rate for the gas phase was 0.052 L/min for packing with the particulate molecular sieve, and the total volume flow rates for gas phase were 0.052 and 0.046 L/min for packing with the staggered molecular sieve membrane respectively. As in the test in the microbalance adsorption system, the temperature was also maintained at room temperature (23-27 °C). Inlet and outlet concentrations of carbon dioxide were recorded continuously, and the adsorption capacity could be obtained. The amounts of carbon dioxide adsorbed by the adsorption system packed with a particulate molecular sieve and by that set by staggered alumina carriers coated with the molecular sieve membrane were also compared. Considering future application and regeneration time for a molecular sieve, the molecular sieve synthesized by the surfactant quaternary ammonium salts with a carbon chain 14 was selected to discuss adsorption performance in the adsorption system.

In addition to carbon dioxide, a molecular sieve can also adsorb many volatile organic compounds. Since methane has high affinity with the adsorbent and does not react chemically with carbon dioxide at normal temperature, methane was chosen as the other adsorbate to investigate the effects of a non-target adsorbate on the carbon dioxide adsorption capacity of the adsorption system. Following the operation conditions described above, the concentrations of both carbon dioxide and methane were controlled at 5.00 μmol/min, and the volume flow rate for the gas phase was controlled at 0.046 L/min. The operating temperature was maintained between 23 and 27 °C.

Molecular sieve characterization

For determination of the surface properties of the molecular sieve, the manufactured molecular sieve particle and membrane were analysed with a Micromeritics particle size analyser, ASAP 2000. Nitrogen was used to detect the pore size, specific surface area and pore structure. Non-linear density function theory (NLDFT) was used to obtained mesopore and micropore volumes. Software ASAP 2010 V.4.00 and DFT V.1.03 were used for control and analysis.

Powder X-ray diffraction (PXRD) was used to identify the structure of the molecular sieve. When X-rays were scattered by a regular crystal, interference phenomena resulting from the scattered light would produce diffraction. Bragg's law was used as a build-in program in the XRD analyser to calculate the unit cell parameters and to report the intensity of the diffraction signal. The type of PXRD used in this study was MAC science 18MPX powder diffraction, and the incident was CuKα radiation. The operating voltage was 40 kV, and the current was 200 mA. The powder was spread on a glass plate homogeneously, and then the plate was placed in the XRD analyser. The scanning speed was 0.5 °/min, the scan step was 0.02°, and the scanning range was from 0.5 to 3°.

In order to compare the difference between the synthesized molecular sieve with and without adding ethanol, the morphology of molecular sieve was observed by JEOL scanning electron microscope, JSM-

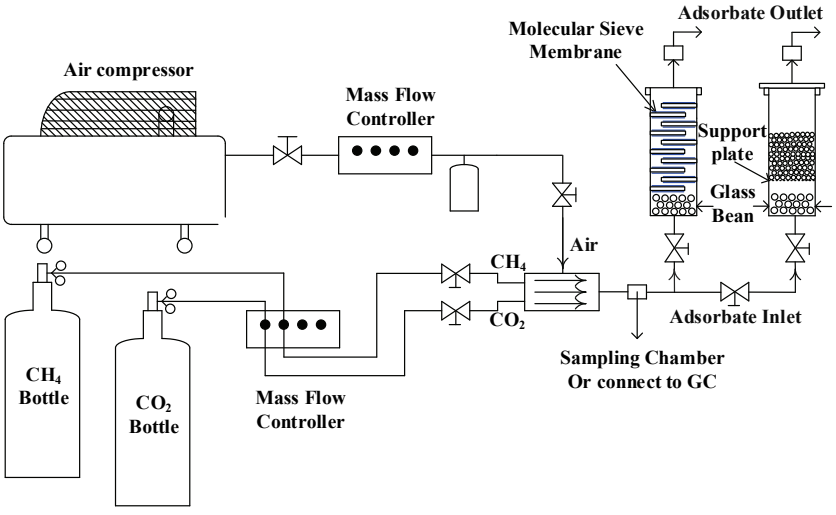

Figure 2. Fixed-bed adsorption system.

-7000F. The operating voltage was from 5 to 10 kV to identify the morphology of the molecular sieve. Molecular sieve samples were dispersed in an ethanol solution, and shocked for 20 min by ultrasonic shockwaves. After drying at room temperature, the sample was coated with platinum by using a vacuum evaporator. Finally, the sample was fed to SEM with 30 kV accelerating voltage to obtain the morphology image.

RESULTS AND DISCUSSION

Data verification

Figure 3 compares the adsorption capacity for carbon dioxide adsorbed by the prepared adsorbents in this study with data from previous studies. Data were compared to the experimental data from Belmabkhout *et al.* [26] who used MCM-41 silica to adsorb carbon dioxide at room temperature. The pressures controlled by Belmabkhout *et al.* [26] ranged from 0 to 25 bar, so only the adsorption data from 0 to 1.8 MPa were adopted in the present study. As shown in Figure 3a, the adsorption capacities for adsorption of carbon dioxide by MCM-41 conducted by Belmabkhout *et al.* [26] was less than those in this study below 1.2 MPa. Although the surface area for the adsorbent prepared by Belmabkhout *et al.* [26] was larger than that in this study, the adsorption capacities in this study were larger than those conducted by Belmabkhout *et al.* [26], which might result from the differences in adsorption equipment and preparation process. Activated carbons honeycomb-monoliths were used by Vargas *et al.* [27] to adsorb carbon dioxide, and the data with similar specific surface area (845-1020 cm^2/g) were examined in comparison with this study. The adsorption capacities in this study were higher than those from Vargas *et al.* [27] The results of the above comparison demonstrate the success of the design of the adsorption system and the preparation of adsorbent in this study, and the following issues are discussed.

The adsorption tests for CO_2 and CH_4 were conducted respectively to acquire the separation factors and the adsorption isotherms for CO_2 and CH_4 are shown in Figure 3b. The microporous and mesoporous adsorbents were prepared by using short carbon-chain quaternary ammonium salts (C-6) and long carbon-chain quaternary ammonium salts (C-14) as surfactant, respectively. The adsorption data were fitted by the Langmuir isotherm as follows:

$$q = \frac{q_m K_a (p_e / p)}{1 + K_a (p_e / p)} \quad (1)$$

where q is the adsorption uptake (mg/g), q_m is the complete monolayer (mg/g), K_a is the adsorption equilibrium constant, p_e is the equilibrium pressure, and p is the total pressure. Therefore, the separation factor K_R found from [28] could be modified as:

$$K_R = \frac{1}{1 + K_a (p_0 / p)} \quad (2)$$

where p_0 is the initial pressure. The parameters K_a and q could be obtained from regressing data by the Langmuir isotherm. The acquired K_a and q_m for the mesoporous adsorbents were 53 and 376 for CO_2 and 22 and 121 for CH_4. Therefore, the separation factors were in the range from 0.021 to 0.727 for CO_2 and in the range from 0.048 to 0.817 for CH_4. Similarly, the separation factors for the microporous adsorbent were in the range from 0.013 to 0.686 for CO_2 and from 0.032 to 0.759 for CH_4. The results demonstrated that both CO_2 and CH_4 were favorably adsorbed by molecular sieve due to the separation factor smaller than 1, and the affinity between the molecular sieve and CO_2 was larger than that between CH_4 and the molecular sieve. Since the adsorbent with the larger pore size would decrease the difference in adsorption capacity for the different adsorbates adsorbed by the adsorbent, the difference in adsorption capacity between CO_2 adsorbed by the molecular sieve and CH_4 adsorbed by the molecular sieve was more significant for the microporous adsorbent, as shown in Figure 3b.

Effect of chain length on molecular sieve

Theoretically, the closer the space between the pore and carbon dioxide, the better the adsorption performance. However, factors that determine an appropriate adsorbent include surface area, pore size, regeneration time, and physical and chemical properties between adsorbent and adsorbate. Whether a material becomes a suitable adsorbent should be determined through the experimental procedure.

Mesoporous adsorbent materials were applied to carbon dioxide adsorption, such as silicon, MCM--41 (mobile composite of matter) and SBA-15 (Santa Barbara Amorphous). Moderate pore size (2-50 nm) and volume for mesoporous materials made carbon dioxide having a better mass transfer rate, thereby enhancing the efficiencies of adsorption and desorption processes. Besides, mesoporous adsorbents could be modified by alkanolamine or amine groups to promote the adsorption of carbon dioxide. For example, studies about mesoporous silica modified by polyethyleneimine (PEI) to enhance CO_2 adsorption capacity and to extend adsorption temperature

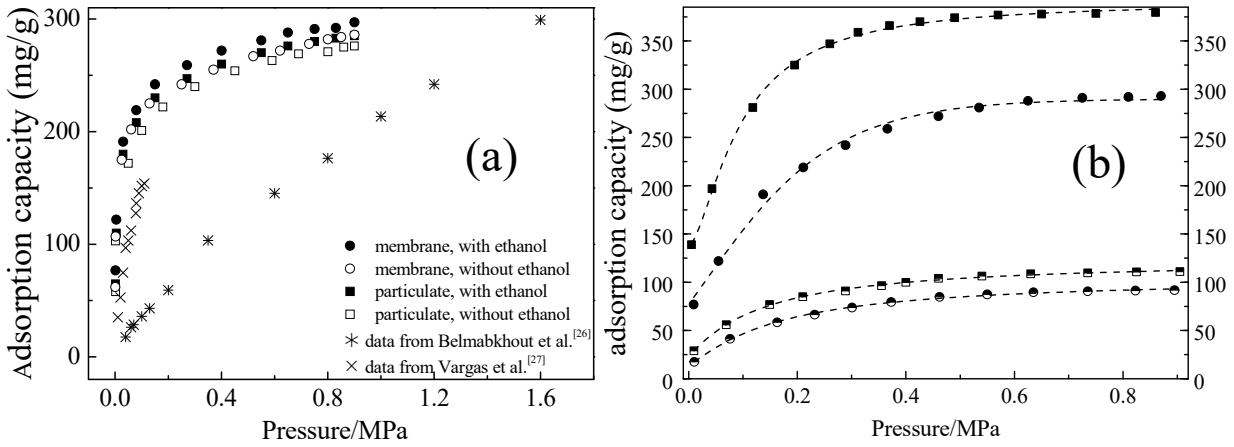

Figure 3. a) Adsorption isotherms in this study and compared with literature data. b) Adsorption isotherm for CO_2 and CH_4 respectively. ● means adsorption of CO_2 on mesopore; ■ means adsorption of CO_2 on micropore; ◓ means adsorption of CH_4 on mesopore; ◨ means adsorption of CH_4 on micropore.

were discussed by MJ *et al.* [29]. In order to separate carbon dioxide from gaseous streams efficiently, polyethyleneimine was loaded into mesoporous molecular sieve MCM-41 by Xu *et al.* [30]. In addition, different types of PEI were investigated to further improve the carbon dioxide adsorption separation performance. The surface modification was not focused; however, adsorption capacity and desorption time were considered in this study. The mesoporous molecular sieve with a smaller pore size (2.75–4.66 nm) was prepared in this study.

In order to investigate the effect of carbon-chain length on the molecular sieve, short carbon-chain quaternary ammonium salts (C-6, C-8) and long carbon-chain quaternary ammonium salts (C-14, C-16) were used as surfactants to prepare the molecular sieve, respectively. After the molecular sieves were synthesized, the surface properties of those were measured by ASAP 2000 analyzer. In addition, non-linear density function theory (NLDFT) was used to obtain mesopore and micropore volumes. Tables 1 and 2 show molecular sieve characteristics obtained from ASAP 2000 analyzer and adsorption data obtained from the microbalance adsorption system. The results show that the pore size increased with the length of the carbon-chain. Although a better adsorption capacity for a molecular sieve with more micropores was concluded from Tables 1 and 2, factors including specific surface area, pore size, and reversibility between adsorption and desorption should be considered in choosing an adsorbent with a suitable pore size. Therefore, several studies related to the adsorption of carbon dioxide by a mesoporous molecular sieve have been published. [6,31-35] As the molecular sieve membrane was prepared under the conditions of hydrothermal temperature 45 °C and addition of ethanol, Figure 4 showed the regeneration curves for carbon dioxide desorbed from molecular sieve membrane at 70 °C. Although the capacity of the more mesoporous molecular sieve synthesized from the longer carbon-chain was lower than that of the more microporous molecular sieve synthesized from the shorter carbon-chain, Figure 4 showed that the additional 30-40 min were required for the more microporous molecular sieve to regenerate completely. Considering future application and regeneration time for a molecular sieve, the surfactant quaternary ammonium salts with a carbon-chain 14 was selected as a major surfactant to discuss adsorption performance in the adsorption system.

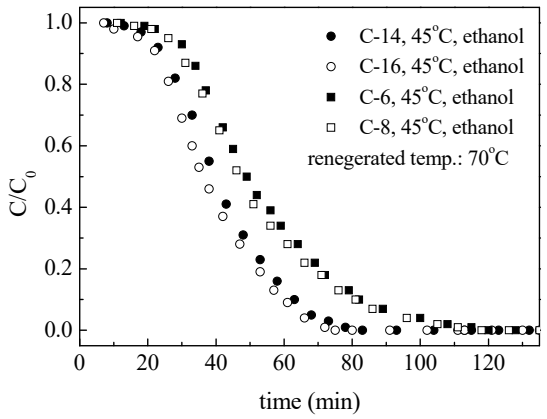

Figure 4. Regeneration curves for carbon dioxide desorbed from molecular sieve membrane at 70 °C.

Effect of hydrothermal temperature on surface properties

The hydrothermal temperature was controlled at 45, 70 and 100 °C to examine the effect of hydro-

thermal temperature on the surface properties of the molecular sieve. The surface properties of the molecular sieves are shown in Tables 1 and 2. A larger pore size was obtained with a higher hydrothermal temperature. As shown in Figure 5, a higher hydrothermal temperature led to a narrower distribution of the pore size and the distribution of the pore size was more homogeneous; however, the molecular sieve with the smaller pore size and the larger surface area was produced from a lower hydrothermal temperature. Therefore, the tests of adsorption isotherms and breakthrough curves for molecular sieves were prepared at 45 °C.

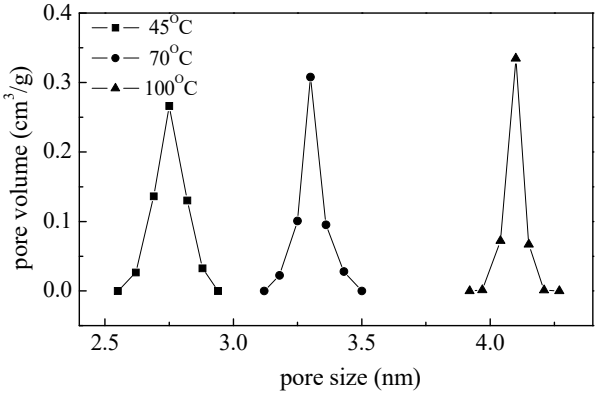

Figure 5. Effect of hydrothermal temperature on distribution of pore size for molecular sieve membrane used C-14 quaternary ammonium salts.

Effect of addition of ethanol on the structure of molecular sieve

It has been reported that the rate of hydrolysis of a surfactant can be increased to prepare spherical particles with a shorter spiral intercept [36,37]; that is, the particles will be close to the circle particulate. As mentioned above, the appearance of a molecular sieve is dependent on the rate of hydrolysis of the surfactant. Their experimental results demonstrated that adding ethanol reduces the rate of hydrolysis and the condensation of surfactant. They used XRD diffraction spectra to prove these phenomena, and the structure c2mm was converted to the structure Ia3d by adding ethanol to the surfactant solution. Figure 6 shows the XRD diffraction spectra for the particulate molecular sieve using C-14 as surfactant solution with addition of ethanol from 0 to 0.75 g at the hydrothermal temperature 45 °C. The surfactants were initially in the interface between aqueous solution and gas phase, and then micelles were formed from surfactants when the amount of surfactant exceeded the critical capacity in the interface. Because of the hydrophilic and hydrophobic properties of ethanol, ethanol would be located between the micellar hydrophilic end and micellar hydrophobic end as ethanol was added to the quaternary ammonium salts aqueous solution. This behaviour would reduce curvature of the micelles, and the structural conversion from c2mm to Ia3d could be demonstrated by XRD analysis. Figure 6 showed that the structure c2mm was observed in the absence of ethanol, and two diffraction signals (20,11) were closer when ethanol was added. When the amount of ethanol was increased, the diffraction signal 20 was more significant and the diffraction signal 11 was shifted to the right until the two signals combined together. The diffraction signal was split into two signals when the amount of ethanol was 2 wt.% (0.6 g), and the structure Ia3d could be found. Since the XRD pattern did not change until the amount of ethanol exceeded 0.6 g, this amount was used for molecular sieve fabrication. Figure 7a shows the SEM image for the particulate molecular sieve using C-14 as surfactant solution without adding ethanol at the hydrothermal temperature 45 °C. As shown in Figure 7a, the spherical particles were obtained. Figure 7b shows the SEM image for the particulate molecular sieve using C-14 as surfactant solution with adding 0.6 g ethanol at the hydrothermal temperature 45 °C . Since the rate of hydrolysis and condensation of surfactant were reduced when the surfactant solution contained ethanol, the short-cylindrical particles developed.

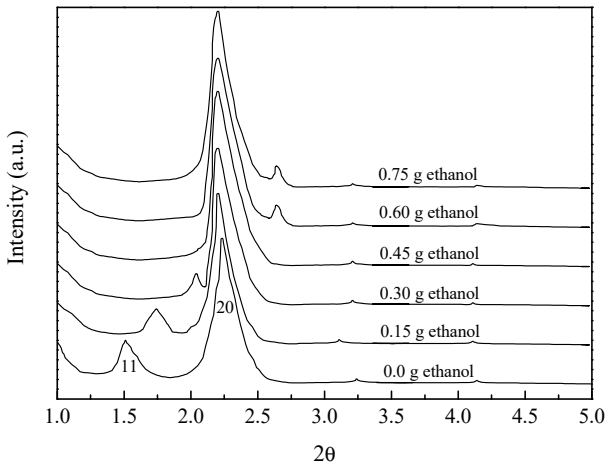

Figure 6. XRD pattern for the particulate molecular sieve using C-14 as surfactant solution with addition of ethanol from 0 to 0.75 g.

Mentioned above, the surface tension is a result of self-cohesion. The porosity in the microstructure might result from lower self-cohesion during formation of the molecular sieve. Therefore, the surface properties, including surface area, mesopore volume,

and micropore volume, were increased with the addition of ethanol as shown in Tables 1 and 2. Most of the resulted porosities contributed to the micropore in the structure, and the increases in mesopore volume for the molecular sieve membrane and particulate molecular sieve were limited. Therefore, the increase in surface area could be attributed to the increase in micropore volume, thus resulting in a larger amount being adsorbed. Since the mesopore was the majority for using C-14 and C-16 as surfactant, the change in surface area and adsorption amount were smaller than those for using C-6 and C-8 as surfactant.

As mentioned above, the rate of hydrolysis and condensation of surfactant would be reduced by the addition of ethanol, and the appearance of the molecular sieve would also change. Therefore, the addition of ethanol was also regarded as a preparation variable. SEM images for molecular sieve membrane used C-14 as surfactant solutions with and without ethanol added are shown in Figure 7c and d, respectively. The structure of the molecular sieve membrane in Figure 7c is the denser of the two, and the structure shown in Figure 7d is looser and exhibits some cracking. This result could be attributed to the fact that adding ethanol reduces the rate of hydrolysis and condensation, which decreases the self-cohesion for the micelle. The lower self-cohesion should facilitate cross-linking between micelles, and the dense molecular sieve membrane was formed.

Adsorption test

The carbon dioxide adsorption capacities for molecular sieves using C-14 as surfactant with and without addition of ethanol were measured by the microbalance adsorption system, and the results are shown in Figure 3a. Since the surface areas for molecular sieve using C-14 as surfactant with addition of ethanol were larger than those without addition of ethanol, the adsorption isotherms with addition of ethanol were also higher than those without addition of ethanol. As shown in Tables 1 and 2, the surface areas for the molecular sieve membrane were larger than that for the particulate molecular sieve, thus Figure 3a shows that the adsorption isotherms for the molecular sieve membrane were higher than that for the particulate molecular sieve. In spite of that, the CO_2 adsorbed by the particulate molecular sieve and molecular sieve membrane shown in Figure 3a were favourable. The result means that the adsorption capacity increases significantly at low pressure, and the affinity between the adsorbate and adsorbent is good.

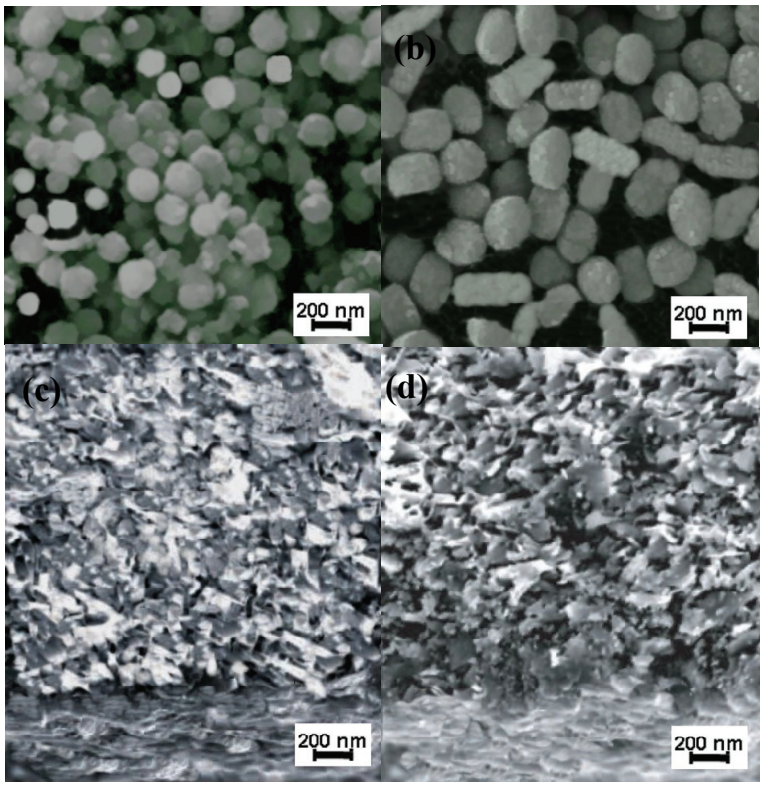

Figure 7. SEM image of particulate molecular sieve using C-14 as surfactant solution without adding ethanol. b) SEM image of particulate molecular sieve using C-14 as surfactant solution with addition of 0.6 g ethanol. c) Cross section of SEM image of molecular sieve membrane with adding ethanol. d) Cross section of SEM image of molecular sieve membrane without adding ethanol.

Generally speaking, the pressure will drop as the gas stream flows through a packed bed, and as a result, the outlet gas flow rate will be less than the inlet gas flow rate. The more closely packed the material is, the larger the pressure drop will be. In order to compare the breakthrough curves of the molecular sieve membrane and particulate molecular sieve reasonably, the weights of the molecular sieve membrane and particulate molecular sieve used in the adsorption tower were the same, 30 g. The weights of the molecular sieve membrane did not include alumina carriers for testing in the fixed-bed adsorption system. For the breakthrough curve, the adsorption performance is better for the longer breakthrough time, and the curve from breakthrough time to $C/C_0 = 1$ is steeper. Comparing solid square and solid circular points in Figure 8a (the same inlet gas flow rate) revealed that the adsorption performance for particulate molecular sieve was better than that for molecular sieve membrane. The surface area presented in Tables 1 and 2 and adsorption isotherms presented in Figure 3a showed that the adsorption capacities for the molecular sieve membrane were better than those for the particulate molecular sieve; however, the particulate molecular sieve was closely packed in the fixed-bed adsorber, which led carbon dioxide to being adsorbed efficiently. Therefore, the breakthrough time and steepness of the breakthrough curve for the particulate molecular sieve with the addition of ethanol was better than others.

The outlet gas flow rate for the adsorption tower packed with the particulate molecular sieve was lower than that of the tower set by alumina carriers coated with the molecular sieve membrane. Since gas flow rate would be affected by the drop in pressure, the difference between inlet and outlet gas flow rates for the particulate molecular sieve was larger than that for the molecular sieve membrane. On the basis of the same weights for both adsorbents, it was difficult to control or change artificially the pressure drops for the installed molecular sieve membrane and particulate molecular sieve in the fixed-bed adsorption system. For the air cleaning system, the amount of outlet fresh air was also an important index. In order to obtain the same amount of outlet fresh air as the particulate molecular sieve in the fixed-bed adsorption system, the lower inlet gas flow rate could be used in the adsorption system set by alumina carriers coated with the molecular sieve membrane. Figure 8a shows that the breakthrough curve for the lower inlet gas flow rate (solid triangular points) was steeper and had longer breakthrough time than those for the larger inlet gas flow rate (solid circular points). Although the adsorption performance for the particulate molecular sieve was still better than that for the molecular sieve membrane, the breakthrough curve for the molecular sieve membrane in the lower gas flow rate was closer to that for the particulate molecular sieve than the larger gas flow rate.

Adsorption behaviours for competitive adsorption were also examined with the breakthrough curves in this study. As mentioned in the section “Adsorption test in microbalance and fixed-bed adsorption systems”, methane was mixed with carbon dioxide to conduct the competitive adsorption tests. Breakthrough curves for adsorbing methane and carbon dioxide by packed and staggered fixed-bed adsorption systems are shown in Figure 8b. Comparing Figure 8a and b revealed that the breakthrough time for the competitive adsorption was shorter than that for a single component, and the difference was about 25 min. The result could be attributed to the fact that the breakthrough time was reduced with increasing the total amount of adsorbates under the constant amount of adsorbent. Figure 8b also showed that the rollover, $C/C_0 > 1$, was present for methane in the

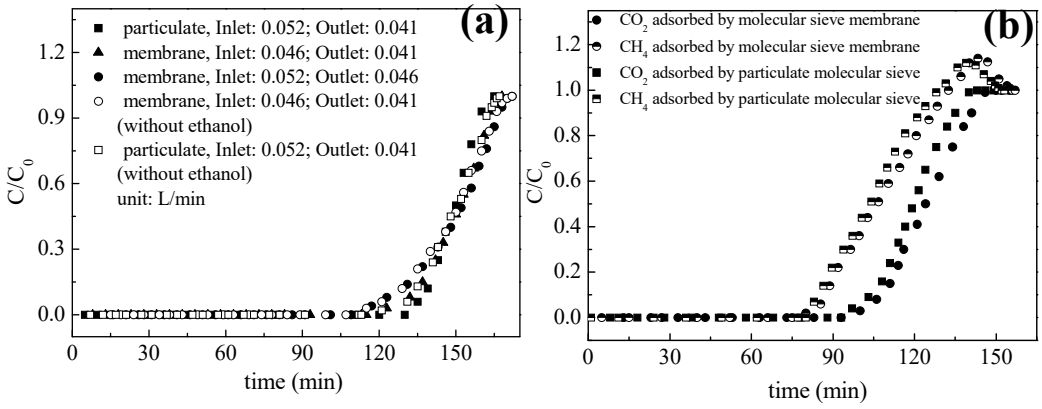

Figure 8. a) Breakthrough curves for carbon dioxide adsorbed by particulate and membrane molecular sieve. b) Breakthrough curves for carbon dioxide and methane adsorbed by packed and staggered fixed-bed adsorption system.

competitive adsorption because methane was displaced by carbon dioxide on the sites of the molecular sieve. Similar to Figure 8a, the breakthrough curves for CO_2 and CH_4 adsorbed by the packed fixed-bed adsorption system (particulate molecular sieve) were better than those by the staggered fixed-bed adsorption system (molecular sieve membrane) due to the closely packed particulate molecular sieve in the fixed-bed adsorber. Since the surface area and adsorption amount for the molecular sieve membrane were larger than those for the particulate molecular sieve, the amounts of adsorbed and desorbed CH_4 were also larger than for the particulate molecular sieve. Therefore, the rollover for CH_4 in the staggered adsorption system was higher than that in the packed adsorption system. The results for breakthrough curves in the competitive adsorption were consistent with adsorption isotherms and surface tests.

CONCLUSIONS

The adsorption isotherms can be obtained quickly from the microbalance adsorption system, and the characteristics of the molecular sieve affected by prepared variables were analyzed. The molecular sieves with the smaller pore size and the larger surface area were found to result from lower hydrothermal temperature. The rate of hydrolysis and condensation of sodium silicate were reduced by the addition of ethanol, and the structure of the molecular sieve membrane was denser. In addition, without the addition of ethanol, the structure of the molecular sieve membrane was looser and exhibited some cracking. Adsorption isotherms showed that the carbon dioxide adsorption capacities of the particulate molecular sieve and the molecular sieve membrane were favourable. On the basis of the same outlet fresh air, the breakthrough curve for molecular sieve membrane in the lower gas flow rate was closer to that for the particulate molecular sieve than the larger gas flow rate. The results for the competitive adsorption not only indicated that the affinity between carbon dioxide and molecular sieve was better than that between the molecular sieve and methane, but also showed that the results for breakthrough curves in the competitive adsorption were consistent with adsorption isotherms and surface tests.

Acknowledgments

The author thanks Tsair-Wang Chung and Ke-Ying Hsu from Chung Yuan Christian University for the analyses and useful discussions about Microbalance, SEM, XRD and ASAP 2000.

REFERENCES

[1] F. Birol, CO_2 Emissions from Fuel Combustion Highlight, IEA Publications. Soregraph, Paris, 2016, p. 11

[2] L. Zhen, C. Shen, F.V.S. Lopes, P. Li, J. Yu, C.A. Grande, A.E. Rodrigues, Sep. Sci. Technol. **48** (2013) 388-402

[3] K.L. Wang, S. Loo, K. Haraya, Ind. Eng. Chem. Res. **46** (2007) 1402-1407

[4] D.M. Nedeljkovic, M.P. Stevanovic, M.Z. Stijepovic, A.P. Stajcic, A.S. Grujic, J.T. Stajic-Trosic, J.S. Stevanovic, Chem. Ind. Chem. Eng. Q. **21** (2015) 277–284

[5] X. Xu, C. Song, B.G. Miller, A.W. Scaroni, Ind. Eng. Chem. Res. **44** (2005) 8113-8119

[6] X. Xu, C. Song, J.M. Andresen, B.G. Miller, A.W. Scaroni, Energy Fuels **16** (2002) 1463-1469

[7] M.A. Ahmad, H. Koris, W.N.H.W. Zainal, Int. J. Eng. Technol. **10** (2010) 101-104

[8] K.S. Liao, Y.J. Fu, C.C. Hu, J.T. Chen, Y.H. Huang, M.D. Guzman, S.H. Huang, K.R. Lee, Y.C. Jean, J.Y. Lai, J. Phys. Chem., C **117** (2013) 3556-3562

[9] S.K. Ghadiri, R. Nabizadeh, A.H. Mahvi, S. Nasseri, H. Kazemian, A.R. Mesdaghinia, S. Nazmara, Iran. J. Environ. Health Sci. Eng. **7** (2010) 241-252

[10] A.T. Shah, B. Li, S.A. Nagra, Can. J. Chem. Eng. **89** (2011) 1288-1295

[11] J.L.H. Chau, C. Tellez, K.L. Yeung, K. Ho, J. Membr. Sci. **164** (2000) 257-275

[12] K. Li, Z. Tian, X. Li, R. Xu, Y. Xu, L. Wang, H. Ma, B. Wang, L. Lin, Angew. Chem. Int. Ed. **51** (2012) 4397–4400

[13] T. Namba, EP 0674939 A2 (1995)

[14] H.H. Funke, M.G. Kovalchick, J.L. Falconer, R.D. Noble, Ind. Eng. Chem. Res. **35** (1996) 1575-1582

[15] M. D. Jia, K.V. Peinemann, R.D. Dehling, J. Membr. Sci. **82** (1993) 15-26

[16] F. Kapteijin, W.J.W. Bakker, J.A. Moulijn, Catal. Today **25** (1995) 213-218

[17] Y.H. Ma, S. Xiang, US 5258339 A (1993)

[18] M. Kazemimoghadam, J. Water Environ. Nanotechnol. **1** (2016) 45-53

[19] Z. Huang, H.M. Guan, W.L. Tan, X.Y. Qiao, S. Kulprathipanja, J. Membr. Sci. **276** (2006) 260-271

[20] S.A. Zygmunt, B.L. Bootz, A.W. Miller, L.A. Curtiss, L.E. Iton, in Proceedings of 17th North American Catalysis Meeting, Toronto, Canada, 2001, p. 2

[21] D. Uzio, J. Peureux, J.A. Dalmon, J.D.F. Ramsay, Stud. Surf. Sci. Catal. **87** (1994) 411-418

[22] H.P. Lin, S.F. Cheng, C.Y. Mou, Chem. Mater. **10** (1998) 581-589

[23] H.P. Lin, Y.R. Cheng, C.Y. Mou, Chem. Mater. **10** (1998) 3772-3776

[24] C.Y. Mou, H.P. Lin, Pure Appl. Chem. **72** (2000) 137-146

[25] C.M. Wang, T.W. Chung, C.M. Huang, H. Wu, J. Chem. Eng. Data **50** (2005) 811-816

[26] Y. Belmabkhout, R. Serna-Guerrero, A. Sayari, Chem. Eng. Sci. **64** (2009) 3721-3728

[27] D.P. Vargas, L. Giraldo, J.C.M. Pirajan, Int. J. Mol. Sci. **13** (2012) 8388-8397

[28] Y.S. Ho, R. Malarvizhi, N. Sulochana, J. Environ. Prot. Sci. **3** (2009) 111-116

[29] M.J. Al-Marri, K.A. Al-Saad, M.A. Saad, D.J. Cortes, M.M. Khader, J. Phys. Chem. Biophys. 7 (2017).

[30] X. Xu, B. Graeffe, C. Song, Prepr. Pap.-Am. Chem. Soc., Div. Fuel Chem. **49** (2004) 259-260

[31] N. Stoeva, I. Spassova, D. Kovacheva, G. Atanasova, M. Khristova, Bulg. Chem. Commun. **48** (2016) 120-124

[32] Y.J. Heo, M.U.T. Le, S.J. Park, Int. Carbon Lett. **18** (2016) 62-66

[33] M.B. Yue, L.B. Sun, Y. Cao, Z.J. Wang, Y. Wang, Q. Yu, J.H. Zhu, Microporous Mesoporous Mater. **114** (2008) 74--81

[34] J. Wei, J. Shi, H. Pan, W. Zhao, Q. Ye, Y. Shi, Microporous Mesoporous Mater. **116** (2008) 394-399

[35] Z. Zhang, W. Zhang, X. Chen, Q. Xia, Z. Li, Sep. Sci. Technol. **45** (2010) 710-719

[36] H.P. Lin, C.P. Kao, C.Y. Mou, Microporous Mesoporous Mater. **48** (2001) 135-141

[37] W.Q. Wang, J.G. Wang, P.C. Sun, D.T. Ding, T.H. Chen, J. Colloid Interface Sci. **331** (2009) 156-162.

HONDA WU

Department of Fashion styling and Design, Chungyu University of Film and Arts, Keelung, Taiwan, R.O.C.

NAUČNI RAD

ADSORPCIJA UGLJEN-DIOKSIDA U ADSORBERIMA SA PAKOVANOM PARTIKULARNIM I CIK-CAK RASPOREĐENIM MEMBRANSKIM MOLEKULSKIM SITIMA

Za uklanjanje ugljen-dioksida je primenjen adsorber sa nepokretnim slojem. Adsorpcione izoterme su dobijene iz uravnoteženog sistema. Analizirane su karakteristike molekulskog sita pri različitim operativnim uslovima. Adsorbenti, uključujući partikularno ili membransko molekulsko sito, korišćeni su za adsorbovanje ugljen-dioksida u adsorberu sa nepokretnim slojem. S obzirom da su površinske osobine molekulskog sita bile pod uticajem uslova njihove pripreme, sintetisana su partikularna i membranska molekulska sita i ona korišćena za proučavanje efekata uslova pripreme na adsorpciju ugljen-dioksida. Rezultati eksperimenta pokazali su da je veličina pora molekulskog sita povećana većom dužinom lanca kvarternih amonijumovih soli i višom temperaturom hidrotermalnog tretmana. Adsorpcione izoterme za ugljen-dioksid adsorbovanim partikularnim ili membranskim molekulskim sitom su bile povoljne. Osim toga, kriva proboja za manji ulazni protok gasa bila je bliža krivoj proboja za partikularno molekulsko sito pri istoj količini izlaznog svežeg vazduha. Rezultati su pokazali da vredi razvijati adsorber sa nepokretnim slojem čestica alumine premazanih membranskim molekulskim sitima.

Ključne reči: adsorpcija, ugljen-dioksid, mikroravnoteža, molekulsko sito, regeneracija.